Int J Thermophys (2008) 29:2126–2135
DOI 10.1007/s10765-007-0305-9

Experimental Study of Gas–Liquid Two-Phase Flow in Glass Micromodels

B. Gutiérrez · F. Juarez · L. Ornelas · S. Zeppieri · A. López de Ramos

Published online: 2 November 2007

Abstract To estimate the most important flow variables in reservoir engineering, such as the relative permeability, it is required to know with high precision, other variables such as saturation, pressure drop of each phase, and porous media data such as porosity and absolute permeability. In this study, experimental tests were performed inside a glass micromodel using gas–liquid two-phase flow in steady-state conditions. The liquid-phase flow and the pressure drop of the porous media were determined. Additionally, the flow development inside the porous media was visualized using a high-speed video camera system. These pictures were recorded at 500 fps, and they were used to compute the phase saturation and the gas velocity in the glass micromodel. The visualization was performed in three regions of the glass micromodel demonstrating that saturation gradients were not present. The effect of the capillary number was studied over the gas–liquid relative permeability curves and on the flow mechanisms. It was concluded that high flow rates minimize edge effects, that the capillary number modifies the relative permeability values and the flow patterns inside the micromodel, and that the high-speed visualization is an efficient and accurate technique to determine saturation values and to study the flow patterns in transparent porous media such as glass micromodels.

Keywords Capillary number · Flow patterns · Gas–liquid two-phase flow · Glass micromodel · Relative permeability · Visualization

B. Gutiérrez (✉) · S. Zeppieri · A. López de Ramos
GFT_{USB} Department of Thermodynamics and Transference Phenomena, University Simón Bolívar, 89000 Caracas, Venezuela
e-mail: bgutierrez@usb.ve

F. Juarez · L. Ornelas
University Simón Bolívar, 89000 Caracas, Venezuela

1 Introduction

Multiphase flows through porous media, in particular two-phase flow, are present in many engineering processes such as oil production and enhanced oil recovery (EOR). Since the beginning of the 20th century, Darcy's law has been generalized to multiphase flows through porous media using the relative permeability concept and developing several methodologies to determine the fluid flows. According to the flow type, the methodologies are classified according to steady-state and transitory-state experiments. The main difference between the steady-state methodologies [1], such as the Penn State, Hassler, and single-core dynamic method, is the form in which they minimize or eliminate the boundary effect [1,2]. This effect is the result of the discontinuity in the capillary properties at the system exit, which generates a saturation gradient along the porous media. This fact means, consequently, that the relative permeability values obtained correspond to mean saturation values. It is hence of utmost importance to calculate accurately the saturation of the phases, and to guarantee the absence of saturation gradients in the porous media.

The most widely used techniques to determine saturation in porous media are mass balance and gravimetric methods [2–4]. These external techniques allow calculations of mean values, and they do not reflect the possible presence of saturation gradients in the porous media. Another disadvantage of these techniques, especially when they are used with small porous media, is the presence of dead volumes [5]. Other techniques used to measure saturation in porous media are in situ techniques, in which the saturation of the phases is directly determined in the porous media without perturbing the distribution of fluids within the system. These techniques offer greater accuracy and precision than the external techniques [5].

The visualization technique with high-speed video cameras is one of the in situ techniques, which allows determination of both the saturation of the phases and the flow pattern in transparent porous media, hence allowing correlation and verification of the strong influence of the flow mechanisms involved in the relative permeability values [6].

Besides assuming the absence of saturation gradients in porous media, it is often assumed that the configuration of the fluids remains static during steady-state flow conditions. This last assumption signifies that a fluid, when not connected in the media, cannot flow through the porous grid, in which case, the relative permeability of this phase is practically negligible. Recently, various experimental studies [6–9] have used transparent porous media with the purpose of studying the mechanisms at the porous scale. Many of them study liquid–liquid two-phase flow and the particular case of solution gas drive, where the rate of the pressure drop is an important process variable. Therefore, variables such as saturation of the phases, viscosity of the phases, surface tension, and media variables such as wettability and saturation history are meaningful factors [10–12], which should be considered to calculate the relative permeability. The majority of these variables have been studied individually. Recently, it has been shown that the interaction between two fluids (viscous coupling effects) can be important in the case of two-phase flows. Some authors [6,13] have proposed viscous coupling models where they consider these effects, but this phenomenon needs to be studied more widely.

It is very useful to group viscous and capillary forces in a dimensionless number called capillary number. In this study, the capillary number (N_{Ca}) is defined as

$$N_{Ca} = \frac{u\mu}{\sigma} \tag{1}$$

where $u(\mathrm{m} \cdot \mathrm{s}^{-1})$ is the superficial velocity, $\mu(\mathrm{Pa} \cdot \mathrm{s})$ is the viscosity of the wetting phase, and $\sigma(\mathrm{N} \cdot \mathrm{m}^{-1})$ is the surface tension.

Many studies [3,14] have been developed, for which the objective is to determine the influence of the capillary number on the liquid–liquid relative permeability. Some authors [15] have also researched the influence of the capillary number on the curves of two-phase flow relative permeability, focusing their studies on the wettability of the porous media. According to the predominant flow conditions, the viscous or capillary forces will establish the flow pattern predominant in the porous media. Thus, visualization experiments in transparent porous media [6–9] are an excellent way to carry out this type of study.

In this study, experimental tests were designed in a glass micromodel with the objective to determine the influence of the capillary number on the steady-state gas–liquid two-phase flow relative permeability. The saturation of the phases was determined through recorded images in the micromodel. These images were also used in the study of flow patterns in the glass micromodel.

2 Experimental Setup

The experimental setup designed to determine the steady-state relative permeability is shown in Fig. 1. The non-wetting phase used was air coming from a gas cylinder (AC) connected to a pressure regulator (PR). The wetting phase, coming from a storage tank, is regulated with a needle valve (V4). The two-phase flow enters simultaneously to the glass micromodel (GM) and the pressure transducer (T). The pressure drop is registered at the indicator (I). Finally, gravitational forces separate the phases.

Three solutions were used as the wetting phase, and glycerin was used as the viscous agent. The surface tension was modified with a non-ionic surfactant. Physical properties of the wetting phase are shown in Table 1. The boundary effect was minimized using high flow rates in each one of the phases.

The glass micromodel used in this study has 53% porosity and a flow area of $9\,\mathrm{mm}^2$. Both values were determined through the micromodel images. The absolute permeability of the glass micromodel is 18 D (darcy). It is assumed that the micromodel is perfectly wettable for the liquid phase.

2.1 Methodology

Initially, the glass micromodel was saturated with the wetting phase, and the non-wetting phase was injected adjusting the pressure for each test to the prefixed value. In this way, the non-wetting phase displaces the wetting phase, generating the drainage curves. This is developed progressively, increasing the Q_{NW}/Q_W ratio. The

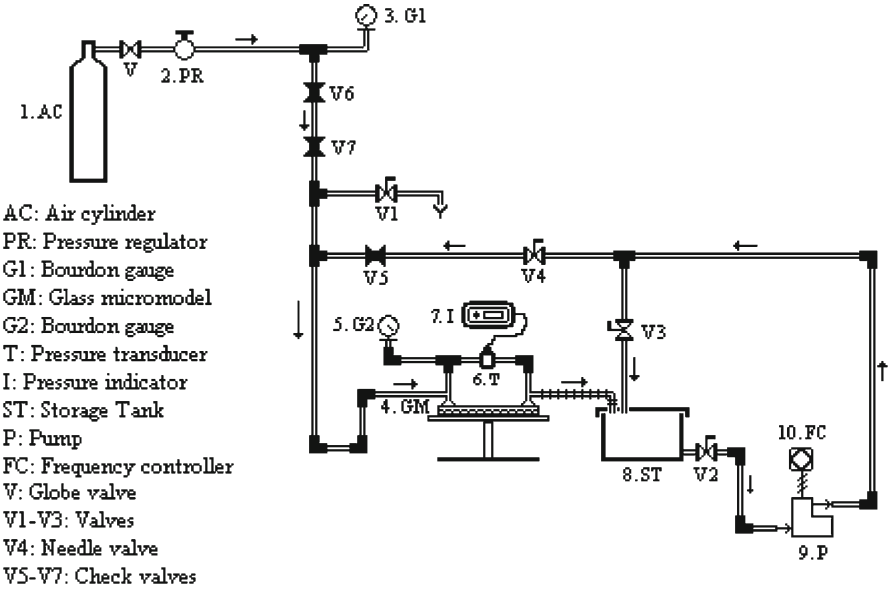

Fig. 1 Experimental setup

Table 1 Physical properties of the wetting phase

		$\rho(\mathrm{kg}\cdot\mathrm{m}^{-3})$	$\mu x 10^3$ (Pa · s)	$\sigma(\mathrm{mN}\cdot\mathrm{m}^{-1})$
Wetting Phase	1	1 150	10	67.6
	2	1 208	40	70.0
	3	1 208	40	46.0

steady-state condition was obtained as soon as the pressure drop in the micromodel was constant. At that moment, the images of the glass micromodel flow were recorded, with the purpose of calculating the saturation of all of the phases.

In the context of this study, it is assumed that the fluids adjust to the isotropic porous media generalized Darcy law:

$$Q_i = \frac{k \cdot kr_i A}{\mu_i}\left(\frac{\mathrm{d}P}{\mathrm{d}x}\right) \quad i : \text{wetting phase, non-wetting phase,} \tag{2}$$

where $Q_i(\mathrm{m}^3\cdot\mathrm{s}^{-1})$ is the flow rate of phase i, $k(\mathrm{m}^2)$ is the absolute permeability of the porous media, $A(\mathrm{m}^2)$ is the cross-section area of the porous media, μ_i(Pa · s) is the viscosity of phase i, $\mathrm{d}P/\mathrm{d}x(\mathrm{Pa}\cdot\mathrm{m}^{-1})$ is the pressure gradient in phase i, and kr_i is the relative permeability to phase i.

Once the steady-flow conditions are established, and the boundary effect is neglected, it can be assumed that the capillary pressure in the micromodel is

uniform, and hence,

$$\Delta P_{\mathrm{W}} = \Delta P_{\mathrm{NW}} \tag{3}$$

Under the assumptions mentioned previously, the liquid flow rate and the relative permeability of the wetting phase, and the gas flow rate and the relative permeability of the non-wetting phase can be related through the following equations:

$$Q_{\mathrm{L}} = \frac{k \cdot kr_{\mathrm{L}} A}{\mu_{\mathrm{L}}} \frac{\Delta P}{L} \tag{4}$$

$$Q_{\mathrm{G}} = \frac{k \cdot kr_{\mathrm{G}} A}{\mu_{\mathrm{G}}} \frac{P_{\mathrm{aver}}}{\sqrt{\frac{P_1^2 + P_2^2}{2}}} \frac{\Delta P}{L} \tag{5}$$

where $P_{\mathrm{aver}} = (P_1 + P_2)/2$.

In this study, the visualization system consisted of a high-speed Kodak Ektapro camera, Model 4540mx Image, a Nikon lens, 60 mm f/2.8D AF Micro-Nikkor, a monitor, and a workstation where the captured images are recorded.

3 Results

Capillary effects were eliminated with high flow rates. The absence of a boundary effect was confirmed with recorded images at three different points of the micromodel, for which saturation of each of the phases was calculated. These calculations were made at three different times (t_1, t_2, and t_3). The gas saturation profile is shown in Fig. 2. In this figure, it can be observed that there is no significant difference concerning the gas saturation values along the micromodel, which verifies the absence of a boundary effect and saturation gradients in the micromodel. Once it was confirmed that the saturation of the phases was constant in the micromodel, the flow was observed exclusively in its central zone.

As mentioned previously, the wetting phase consisted of three diluted glycerin solutions. The physical properties of the wetting phase are shown in Table 1. The surface tension was modified with a non-ionic surfactant. The non-wetting phase used was air.

In Fig. 3, gas–liquid relative permeability curves are shown. In this figure, it can be observed, as expected according to the liquid saturation values in the glass micromodel, than the liquid relative permeability (kr_{L}) is greater that the one corresponding to the gas (kr_{G}). Low values of kr_{G} are a consequence of the assumption that each of the phases flows separately through the micromodel, and therefore, the flow of each phase is inversely proportional to its own viscosity. Furthermore, this fact assumes that the non-wetting phase only flows when it is connected in the porous media. This contradicts the observations made in the glass micromodel. In all experiments, a continuous flow of slug bubbles type (Fig. 4a) was observed for the case where the wetting phase did not contain surfactant, and a flow of dispersed type (Fig. 4b) in the presence

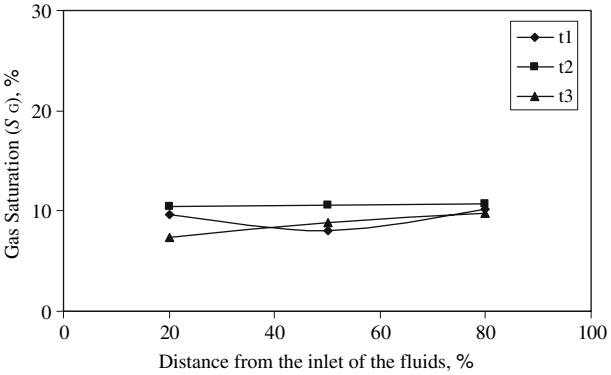

Fig. 2 Saturation profile of the gas phase in the micromodel

of a surfactant. These flow patterns observed in the micromodel confirm the observations reported previously [6,13], where the idea of developing models, for which viscous coupling effects are considered at the moment of calculating the gas–liquid relative permeability, is presented. This fact will be considered in future experiments. Since the experimental equipment was designed to determine the relative permeability at steady-state conditions, the extreme points of those curves could not be determined.

Figure 5 shows relative permeability curves for two different flow patterns observed in the micromodel. As mentioned before, a dispersed flow was observed in the micromodel in the presence of a surfactant; in other words, the reduction in the surface tension increases the interfacial area between the phases, which favors the formation of a large amount of gas bubbles in the liquid. In the absence of a surfactant, a slug flow was observed as a consequence of a higher surface tension. In this last flow pattern, it was observed that the bubbles traveled more slowly than those corresponding to dispersed flow. Figures 5a and 6 show that an increase in the capillary number increases the kr_{L}, which means a higher displacement of this phase through the micromodel. It can be interpreted, from the images of the flow in the micromodel and the increase in kr_{L}, that a flow dominated by viscous forces where a large amount of bubbles is present favors the displacement of the wetting phase through the porous media. In Figs. 5b and 6, it can be observed that kr_{G} increases in slug flow when the capillary number increases due a change on the viscosity of the wetting phase from 40 to 10 mPa · s, but kr_{G} decreases when the observed pattern flow changed from slug flow to dispersed flow and the capillary number increases to 9.3×10^{-4}. This effect was a consequence of the significant increase in the viscous forces in the wetting phase, which increased the resistance of this phase to flow and to let the non-wetting phase flow. The images visualized in these experiments show that the gas phase velocity decreased considerably with the increase in the viscosity of the wetting phase. At higher capillary number, it was observed that many of the gas bubbles remain static in the micromodel prior to their advance, and later exit from the micromodel.

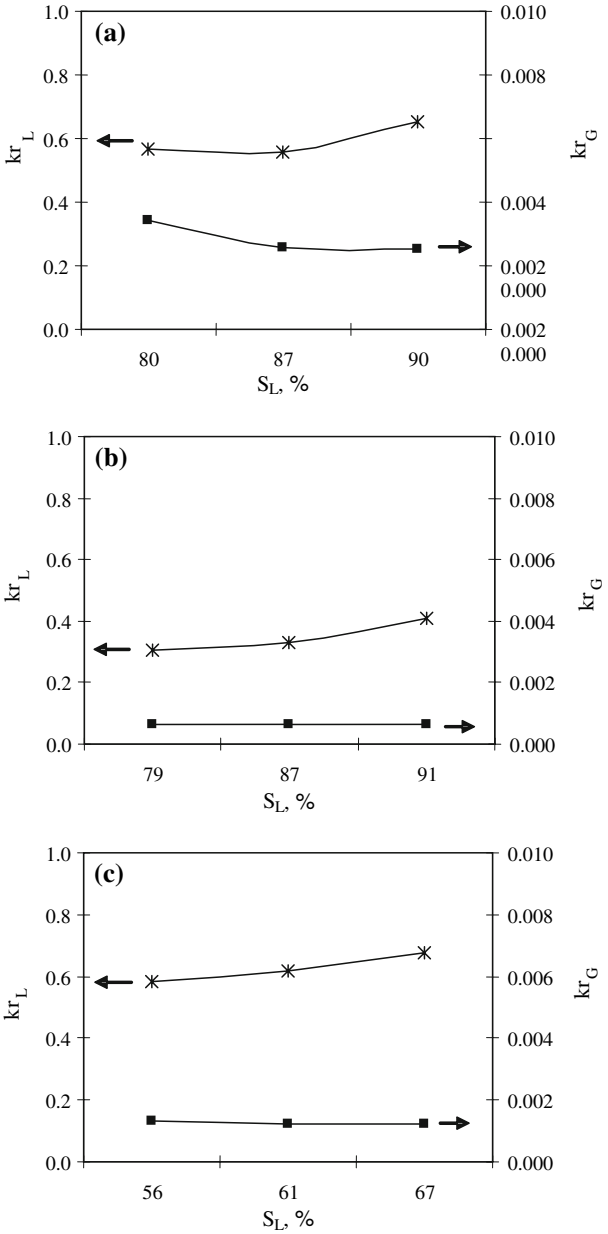

Fig. 3 Gas–liquid relative permeabilities: (**a**) water–glycerin, 10 mPa · s; (**b**) water–glycerin, 40 mPa · s; and (**c**) water–glycerin–surfactant, 40 mPa · s

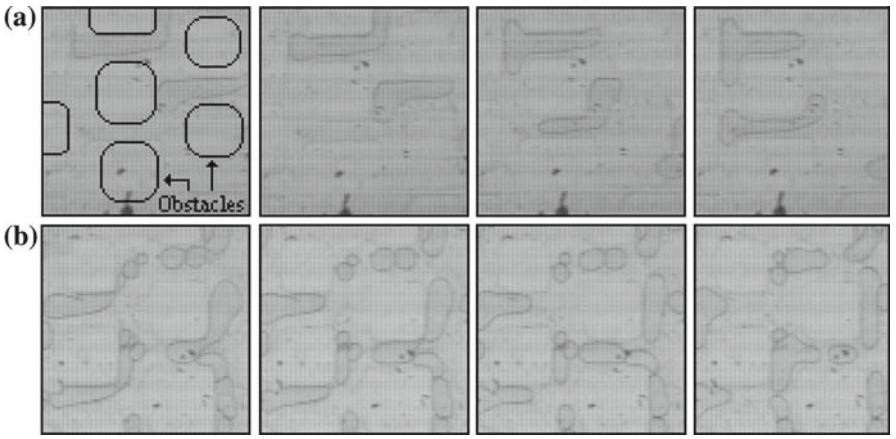

Fig. 4 Flow visualization in the glass micromodel: (**a**) evolution in time of the flow without surfactant: slug flow and (**b**) evolution in time of the flow with surfactant: dispersed flow

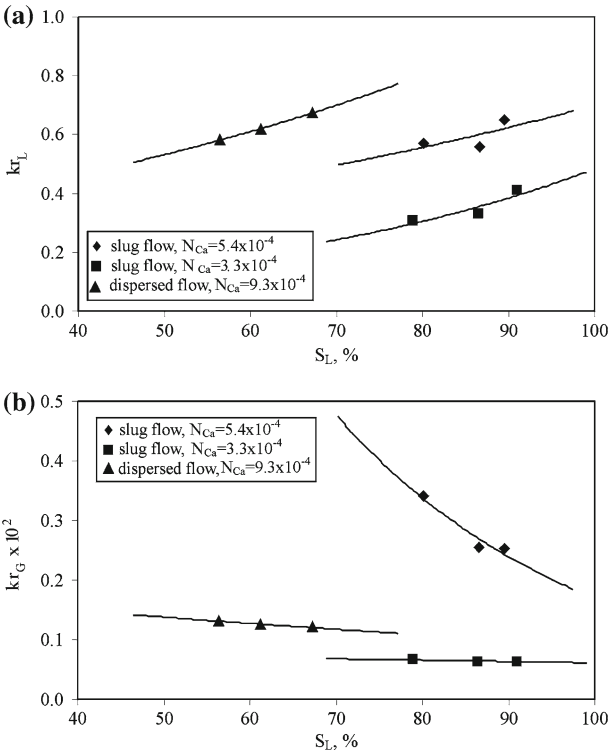

Fig. 5 Relative permeabilities at different capillary numbers and flow patterns: (**a**) liquid relative permeability and (**b**) gas relative permeability

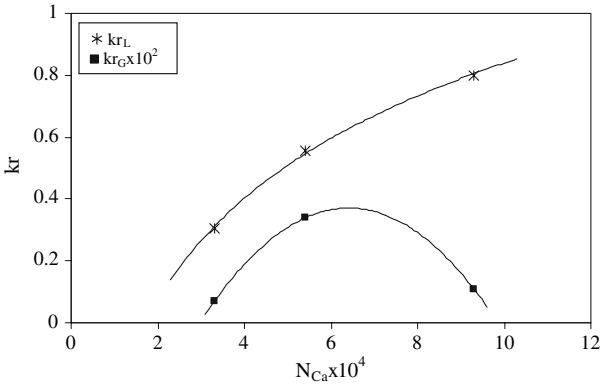

Fig. 6 Relative permeability versus capillary number at $S_L = 80\%$

4 Conclusions

The main conclusions of this study are:

- Visualization with high-speed video cameras is an efficient and accurate in situ technique to determine saturation and verify the absence of saturation gradients in glass micromodels. Besides, this technique can be used to observe and study the flow mechanism inside the porous media.
- Viscous coupling effects are clearly present in gas–liquid two-phase flow in porous media.
- A slug flow was observed for liquid viscosities of 10 and 40 mPa · s in the absence of a surfactant in the wetting phase.
- A dispersed flow was observed for a liquid viscosity of 40 mPa · s when the surface tension was reduced from 70 to 46 mN · m^{-1}.
- Relative permeability of the wetting phase increase with an increase in the capillary number.
- Large gas bubbles present in the flow increases the recovery of liquid flow in porous media.
- Gas–liquid relative permeability values are directly related to the flow mechanism observed in the micromodel.

References

1. J.S. Osoba, J.G. Richardson, J.K. Kerver, J.A. Hafford, P.M. Blair, Trans. AIME **192**, 47 (1951)
2. J.G. Richardson, J.K. Kerver, J.A. Hafford, J.S. Osoba, Trans. AIME **195**, 187 (1952)
3. R.A. Fulcher, T. Ertekin, C.D. Stahi, *SPE 12170* (1983)
4. E. Dana, S. Skoczylas, Int. J. Multiphase Flow **28**, 1719 (2002)
5. M. Honarpour, S.M. Mahmood, SPE Technol. Today Series, *SPE 18565* (1986)
6. D.G. Avraam, A.C. Payatakes, Transport in Porous Media **20**, 135 (1995)
7. M. Lago, R. Gómez, M. Huerta, presented at Petroleum Society's Canadian International Petroleum Conference, Paper 2000–2056, 2000
8. A. Kamp, C. Heny, L. Andarcia, M. Lago, A. Rodríguez, *SPE 69725* (2001)

9. M.A. Theodoropoulou, V. Sygouni, V. Karaoutsos, C.D. Tsakiroglou, Int. J. Multiphase Flow **31**, 1155 (2005)
10. T.M. Geffen, W.W. Owens, D.R Parrish, R.A. Morse, Trans. AIME **192**, 99 (1951)
11. K. Mohanty, Ph.D. Thesis, University of Minnesota, Minneapolis, 1981
12. C.M. Marle, *Éditions Technip* (Paris, 1981)
13. A. Kamp, D.D. Joseph, *SPE 69720* (2001)
14. T.S. Ramakrishnan, D.T. Wasan, *SPE 12693* (1984)
15. S. Ayirala, D. Rao, Colloids Surf. **241**, 313 (2004)